



# Beneficial influences of pelelith and dicyandiamide on gaseous emissions and the fungal community during sewage sludge composting

Jishao Jiang<sup>1</sup> · Youwei Pan<sup>1</sup> · Xianli Yang<sup>1</sup> · Juan Liu<sup>1</sup> · Haohao Miao<sup>1</sup> · Yuqing Ren<sup>1</sup> · Chunyan Zhang<sup>1</sup> · Guangxuan Yan<sup>1</sup> · Jinghua Lv<sup>1</sup> · Yunbei Li<sup>1</sup>

Received: 25 November 2018 / Accepted: 25 January 2019 / Published online: 4 February 2019  
© Springer-Verlag GmbH Germany, part of Springer Nature 2019

## Abstract

Reducing the emissions of NH<sub>3</sub> and greenhouse gases (GHGs) during composting is essential for improving compost quality and controlling environmental pollution. This paper investigates the effects of pelelith (P) combined with dicyandiamide (DCD) on gaseous emissions and the fungal community diversity during sewage sludge (SS) composting. Results showed that the P and P + DCD treatments decreased the cumulative gaseous emissions by 41% and 22% for NH<sub>3</sub>, 21% and 34% for N<sub>2</sub>O, and 31.5% and 33.0% for CH<sub>4</sub>, respectively. The evolution of the fungal community analysis showed that *Ascomycota* and unclassified fungi dominated during the thermophilic stage, while only *Ascomycota* was the dominant fungal phylum during the maturity stage, composing 62%, 66%, and 73% of the total fungal community in the control, P, and P + DCD, respectively. The P and P + DCD significantly increased the fungal community richness at the genus level. Fungal community abundance was found to be significantly related to temperature, pH, organic matter, and total Kjeldahl nitrogen, which also influence the gaseous emissions during SS composting. It suggested that the combined addition of pelelith and dicyandiamide (DCD) was an effective method for reducing the emissions of NH<sub>3</sub> and greenhouse gases during SS composting.

**Keywords** Composting · Pelelith · Dicyandiamide · NH<sub>3</sub> · Greenhouse gases · Fungal community

## Introduction

Composting is an effective and environmental solution for stabilizing and converting the organic waste into a good organic fertilizer or soil conditioner that can be used for agricultural and horticultural applications (Santos et al. 2018; Wang et al. 2018a). However, emissions of greenhouse gases (GHGs; N<sub>2</sub>O, CO<sub>2</sub>, and CH<sub>4</sub>) and ammonia (NH<sub>3</sub>) are inevitable during the composting process (Mao et al. 2018; Sanchez et al. 2015). These gaseous emissions not only reduce the agronomic value of compost but also

significantly contribute to the greenhouse effect and haze formation (IPCC 2007; Pan et al. 2018). Thus, reducing the emissions of NH<sub>3</sub> and GHGs is essential for improving the quality of compost and controlling this type of environmental pollution.

Using bulking agents is considered the most effective and simplest method of reducing NH<sub>3</sub> and GHG emissions, as well as improving the quality of the end compost (Jain et al. 2018; Zhang et al. 2018). Usually, the bulking agents can be divided into three types: carbon-rich substances such as wheat straw, saw dust, biochar, and mushroom dregs (Jiang et al. 2017, 2018; Liu et al. 2017), acidic materials such as sulfuric acid, bamboo charcoal, and nitric acid (Li et al. 2018; Haddadin et al. 2009; Khan et al. 2009), and mineral additives such as medical stone, zeolite, and bentonite. Among these three bulking agents, mineral additives (such as medical stone, zeolite, and bentonite) are the most universal amendments and have been proven to improve the composting process and nutrient conservation. For example, Wang et al. (2018b) investigated that 10% biochar and zeolite could decrease NH<sub>3</sub> emissions by 64.5–74.3% and N<sub>2</sub>O emissions by 79.5–

---

Responsible editor: Philippe Garrigues

✉ Jishao Jiang  
jiangjishao@163.com

✉ Yunbei Li  
liyunbei@163.com

<sup>1</sup> School of Environment, Key Laboratory for Yellow River and Huai River Water Environmental and Pollution Control, Ministry of Education, Henan Key Laboratory for Environmental Pollution Control, Henan Normal University, Xixiang 453007, Henan, China

81.1% during the composting of pig manure and reduce nitrogen and carbon loss. Chowdhury et al. (2014) found that the addition of biochar during the composting of barley straw and hen manure could reduce the total GHG emissions (as CO<sub>2</sub> equivalents) by 27–32%. Chan et al. (2016) noted that adding 10% zeolite and struvite salt during food waste composting could decrease NH<sub>3</sub> emissions by 18–26%.

Pelelith (P), with an approximate formula of Ca<sub>19</sub>(Al, Fe)<sub>10</sub>(Mg, Fe)<sub>3</sub>[Si<sub>2</sub>O<sub>7</sub>]<sub>4</sub>[SiO<sub>4</sub>]<sub>10</sub> (O, OH, F)<sub>10</sub>, is an orthosilicate mineral (Deer 1992). Due to its low density, high total pore volume, and high specific surface area, P has been widely used for removing nitrogen and phosphate from polluted water and as a substrate for the cultivation of microorganisms. In addition, Vesuvianite has also been used in building materials and landscaping due to its properties of being acid-alkali-resistant, lightweight, sound insulating, high hardness, antiskid, and strong resistibility of effloresce and high temperature (Groat 1992; Li et al. 2009). However, no information is available about the influences of P on NH<sub>3</sub> or GHGs during the composting process.

Addition of a nitrification inhibitor (NI) is a well-known and practical approach for reducing N<sub>2</sub>O emissions in farmland ecosystems (Kelliher et al. 2008; Lam et al. 2016). In recent years, many researchers have drawn on the measures used in croplands and added an NI during composting (Zhang et al. 2016a, b). Although the addition of an NI could significantly reduce N<sub>2</sub>O emissions, it would likely increase NH<sub>3</sub> emissions due to the accumulation of ammonium during composting (Zhang et al. 2016b). Thus, researchers have also investigated the influences of applying a combination of an NI and mineral additives, such as struvite crystals and phosphogypsum, on NH<sub>3</sub> and GHG emissions during the composting process (Jiang et al. 2016; Luo et al. 2013).

Composting is a process of microbial community succession that mainly involves bacteria and fungi (Awasthi et al. 2017; Tortosa et al. 2016). However, studies of bacterial communities in composting systems are much more numerous than those of fungal communities in such systems (Mao et al. 2018; Wei et al. 2018). Maintaining a favorable and suitable fungal composition is vital for efficient and successful composting (Wang et al. 2018a); thus, more attention must be paid to the succession of the fungal community. The rapid development of high-throughput sequencing (HTS) has enabled the convenient analysis of the fungal community composition during the composting process (Wang et al. 2018a).

The main objectives of the present study were to (1) compare the effects of a combined addition of P and NI on the emissions of NH<sub>3</sub> and GHGs and the succession of the fungal community during sewage sludge (SS) composting and (2) explore the relationship between environmental factors and the fungal community to identify the critical index reflecting the evolution of fungal species.

## Materials and methods

### Raw materials and additives

Dewatered SS and saw dust (SD) were sampled from a local municipal wastewater treatment plant and a furniture factory in Xinxiang, Henan, China. The SD was the residual material remaining after processing timber and was used as a bulking agent. The SD was pulverized into 1.0–2.0 cm pieces to be readily mixed with SS uniformly. Selected characteristics of the SS and SD are presented in Table 1. The NI used in this study was dicyandiamide (DCD), which was chemically pure and reagent grade. P, with a size of 3–5 mm, was purchased from the online shopping platform Taobao (<https://www.taobao.com/>). The Brunauer-Emmett-Teller (BET) surface area and total pore volume of P were 26.5 m<sup>2</sup> g<sup>-1</sup> and 0.8 cm<sup>3</sup> g<sup>-1</sup>, respectively. An image of the P used is shown in Fig. 1a.

### Composting design and sampling

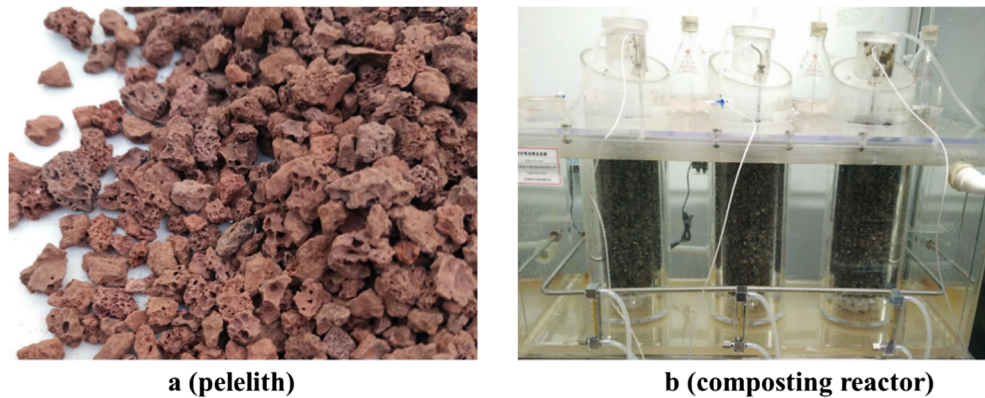
Laboratory-scale composting equipment was used for the composting experiments, and an image of the reactors used, which consisted of a cylindrical polyethylene reactor (with a volume of 14 L, diameter of 20.0 cm, and height of 45.0 cm), a water tank, a heater, an air pump, an air flowmeter, etc., is shown in Fig. 1b. A total of three treatments were conducted: the fresh SS and SD were mixed in a ratio of 1:5 (wet weight), and the two additives were then applied. In the P treatments, P was added at a 15% dry weight basis of the mixture of SS and SD at the beginning of composting. The P + DCD treatment consisted of adding 15% P and 0.5% DCD on a dry weight basis of the SS/DD mixture. Half of the DCD was mixed with the SS/DD mixture in the beginning, and the other half was added during the turning on day 8. A treatment with no additives was used as a control (CK) for comparison. The composting experiments were conducted in the same three cylindrical polyethylene reactors for 20 days. The reactors were placed in a water tank to decrease the heat loss during composting. The temperature of the water bath was set based on the temperature of the compost and maintained below the lowest temperature of the three treatments by 2–3 °C (Meng et al. 2017). Air was pumped by air pumps at the bottom of each reactor at a flow rate of 0.4 L min<sup>-1</sup> during the heating

**Table 1** Properties of the raw materials used in composting

| Raw material | OM (%)     | pH          | Moisture (%) | C/N  |
|--------------|------------|-------------|--------------|------|
| Fresh SS     | 41.8 ± 0.4 | 7.12 ± 0.04 | 81.0 ± 0.23  | 15.6 |
| SD           | 97.2 ± 0.6 | 7.52 ± 0.06 | 8.38 ± 0.04  | 74.7 |

SS, sewage sludge; SD, saw dust; OM, organic matter. The results are the mean of three measurement replicates ± standard deviation

**Fig. 1** Images of P (a) and the composting reactor (b)



**a (peolith)**

**b (composting reactor)**

and thermophilic phases. After the thermophilic phase, the flow rate was set to  $0.2 \text{ L min}^{-1}$ .

Homogeneous compost was sampled on days 0, 2, 4, 8, 12, 16, and 20. The compost samples were divided into two parts: one was stored at  $4 \text{ }^\circ\text{C}$  for more immediate analysis and the other was air dried, passed through a  $0.25 \text{ mm}$  sieve, and stored in a desiccator for later analysis. Fresh compost samples on days 4 and 20 were frozen and sent to Majorbio Bio-Pharm Technology Co., Ltd., China, for 18S rDNA determination.

### Analytical analysis

Compost water extracts with a ratio of 1:10 (*w/w*) were prepared for the determination of pH and dissolved organic carbon (DOC). To determine the DOC content, the compost water extracts were centrifuged at 12000 rpm for 8 min, filtered through a  $0.45 \text{ }\mu\text{m}$  membrane, and then measured by an automated TOC analyzer (Shimadzu TOC-V).  $\text{NH}_4\text{-N}$  in compost-KCl extract (1:10, *v/v*) was detected by NaOH distillation- $\text{H}_2\text{SO}_4$  titration. Total Kjeldahl nitrogen (TN) was determined by the Kjeldahl method (Barrington et al. 2002). Organic matter (OM) was determined from the difference in dry solid mass before and after heating in a muffle furnace at  $550 \text{ }^\circ\text{C}$  for 5 h (Meng et al. 2017).  $\text{NH}_3$  emissions were adsorbed with 2%  $\text{H}_3\text{BO}_3$  and then titrated with HCl (Yang et al. 2015). The three GHGs ( $\text{N}_2\text{O}$ ,  $\text{CO}_2$ , and  $\text{CH}_4$ ) were collected daily in the first weeks and twice a day thereafter and were determined by gas chromatography (Agilent Technologies 7890B Network GC system, China).

### DNA extraction and HTS

DNA was extracted from compost using a MoBio PowerSoil® DNA Isolation Kit according to the manufacturer's protocol. 18S rDNA sequence analysis was carried out with the Illumina MiSeq paired-end 300 bp protocol (Illumina, Inc., San Diego, CA, USA) at Shanghai Majorbio Biotechnology Co. Ltd. (Shanghai, China). The internal transcribed spacer (ITS) regions

of the ribosomal DNA gene were amplified with primers ITS1F (5'-CTGGTCATTTAGAGGAAGTAA-3') and ITS2R (5'-GCTGCGTTCTTCATCGATGC-3'). The raw sequence data were processed in QIIME 1.7.0. The quality-filtered sequences were clustered into operational taxonomic units (OTUs) at a 97% threshold (Edgar 2010; Metcalf et al. 2016).

### Statistical analysis

All environmental parameters were analyzed using SPSS 18.0 software. Graphs were generated with SigmaPlot 12.5 and CANOCO 4.5. Analysis of the fungal community data was conducted using the i-Sanger platform (<http://www.i-sanger.com/>) provided by Majorbio Bio-Pharm Technology Co. Ltd. (Shanghai, China). Six indexes of alpha diversity—the number of OTUs, richness (Chao and Ace), diversity (Shannon and Simpson), and sequencing coverage—were used to assess the microbial diversity and richness. The relative abundances of the dominant phyla and genera were visualized in heat maps and one-way ANOVA bar plots using the i-Sanger platform.

## Results and discussion

### Effect of P and DCD on physicochemical indexes

Figure 2a shows the changes in the temperature profiles during composting. In contrast to other studies, the temperature in all treatments in this study bypassed the temperature of the mesophilic stage and reached that of the thermophilic stage ( $> 50 \text{ }^\circ\text{C}$ ) on day 1. The highest temperatures in the CK, P, and P + DCD treatments, which were all recorded on the 2nd day, were 57.3, 58.5, and 56.4  $^\circ\text{C}$ , respectively. The thermophilic stage was maintained for 8, 8, and 7 days in the CK, P, and P + DCD treatments, respectively; during this stage, the compost should be free of weed seeds and pathogens and satisfy the compost sanitary standard (Kulikowska 2016). During the first 4 days, the temperature in the P treatment

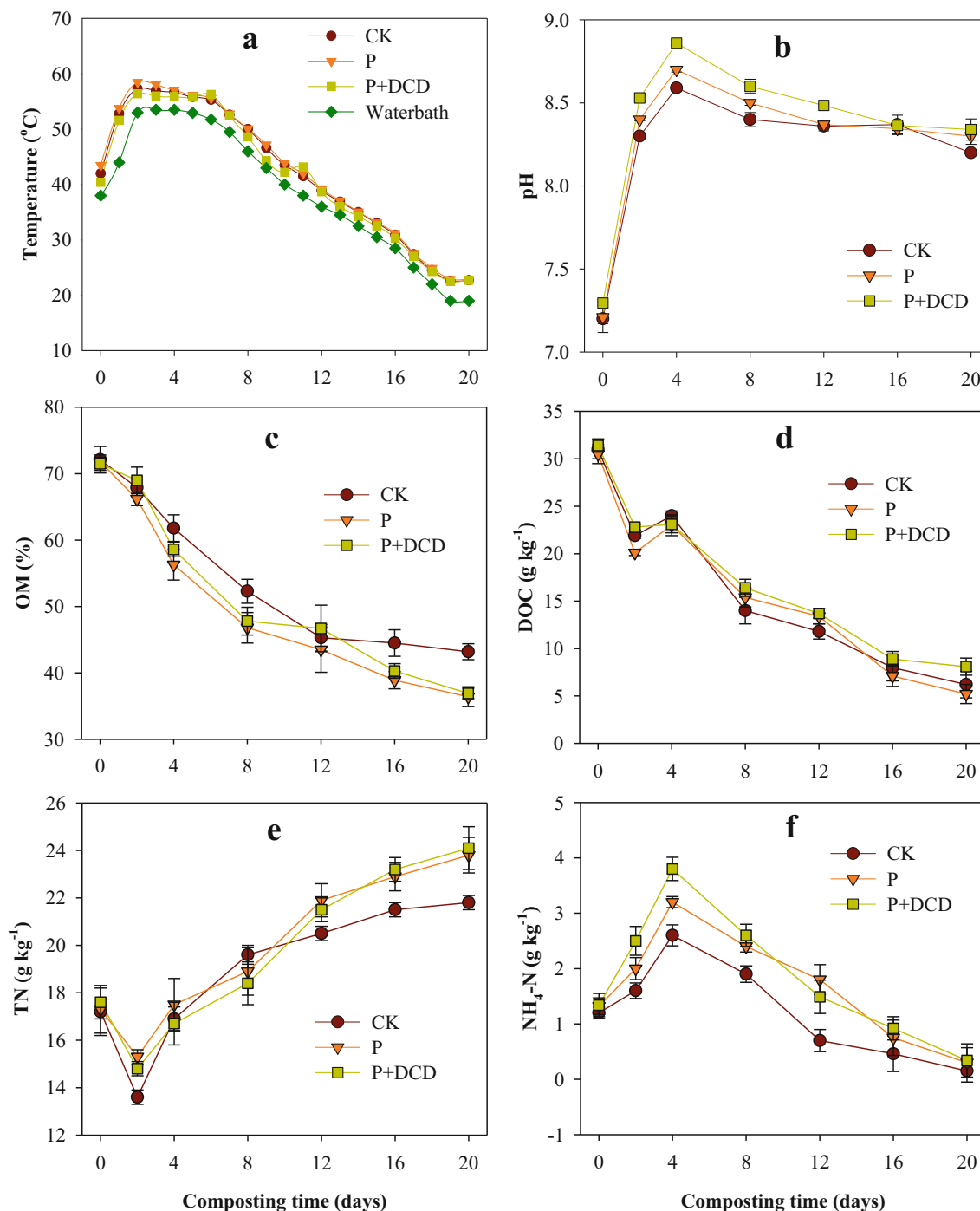


**Fig. 2** Changes in temperature (a), pH (b), OM (c), DOC (d), TN (e), and NH<sub>4</sub>-N (f) during SS composting

was higher than that in the CK treatment, but the temperature in the P+DCD treatment was lower than that in the CK treatment. The possible reason for this difference is that the addition of P-stimulated microbial growth, resulting in rapid OM degradation, but DCD inhibited microbial activities. P, with a high BET surface area and total pore volume, has similar properties to biochar, struvite, medical stone, and zeolite (Awasthi et al. 2018a; Li et al. 2018; Wang et al. 2018b).

Awasthi et al. (2018a) found that the addition of medical stone caused compost to reach the thermophilic stage sooner and attain a higher temperature than that in the control because medical stone addition could increase the porosity and reduce the acidity of the composting mass during the bio-oxidation stage. After the thermophilic stage, the temperature among the three treatments was almost the same and gradually decreased to 20–30 °C.

The pH in the three treatments showed the same trend (Fig. 2b): the pH increased rapidly during the first 4 days, gradually decreased during the days 4–12, and remained at approximately 8.3 during the end of composting. The initial increase in pH was due to the release of ammonium and volatile ammonia from the mineralization of OM (Awasthi et al. 2018a). Afterwards, the volatilization of volatile ammonia and the production of organic acids could explain the reduction in pH (Bernal et al. 2009). Finally, the pH of the end compost was approximately 8.3, which meets the requirements for land application (Bernal et al. 2009). The maximum pH values in the P and P + DCD treatments were 8.70 and 8.86, respectively, which were higher than that in the CK treatment (8.59). This increased pH was probably a result of P absorbing the volatile ammonia during composting, increasing the content of ammonium nitrogen. Moreover, the addition of DCD inhibited nitrification and increased ammonium nitrogen (Zhang et al. 2016b). Wang et al. (2018b) found that the addition of biochar significantly increased the pH compared with that in the control during pig manure and wheat straw composting.

Figure 2c indicates that the OM content in the three treatments decreased rapidly during the first 8 days, especially in the P and P + DCD treatments. Overall, the OM in CK, P, and P + DCD decreased from initial values of 72.1%, 71.8%, and 71.5% to 43.2%, 36.4%, and 36.9%, respectively, corresponding to OM losses of 40.1%, 49.3%, and 48.4%, respectively. As a bulking agent, P has a low density, high total pore volume, and high specific surface area, so its addition could improve the growth of microorganisms and accelerate the degradation of OM (Li et al. 2009). However, DCD inhibits microbial activity; thus, the OM loss in the P + DCD treatment was slightly lower than that in the P treatment, which was also reported in a previous study (Zhang et al. 2016b). The temperature profile also supports this conclusion (Fig. 2a).

Figure 2d shows the change in DOC concentration during composting. The DOC contents in the three treatments rapidly decreased on day 2, which was also found by other researchers (Gomez-Brandon et al. 2008; Wang et al. 2016). This decrease might be because microorganisms preferentially metabolized the available carbon in the compost material during the initial stage (Khan et al. 2014). Afterwards, the degradation of OM produced a large amount of available carbon (Gomez-Brandon et al. 2008), resulting in an increase in DOC. After 4 days, the DOC contents in CK, P, and P + DCD gradually decreased until the end of composting to 6.2, 5.2, and 8.1 g kg<sup>-1</sup>, respectively, which all met the maturity requirement (Bernal et al. 2009).

At the beginning of composting, the TN contents sharply decreased due to ammonia emissions (Fig. 2e). After day 2, TN increased until the end of composting because of the degradation of OM and the related concentration effect. The same results were also reported in previous studies (Jiang et al.

2016; Wang et al. 2016). The final TN contents in the CK, P, and P + DCD treatments were 22.1, 23.8, and 24.1 g kg<sup>-1</sup>, respectively, corresponding to increases of 28.5%, 35.3%, and 33.5% compared with the initial TN contents. This result indicates that the addition of additives exerted a stronger effect on N conservation. P could promote a favorable environment for microbial growth and has an absorption effect (Li et al. 2009). DCD inhibits nitrification and denitrification and reduces the loss of nitrogen gas during composting (Jiang et al. 2016).

NH<sub>4</sub>-N reflects the transformation of nitrogen and is used to assess the maturity of the compost during the composting process (Bernal et al. 2009). As shown in Fig. 2f, the NH<sub>4</sub>-N contents in the CK, P, and P + DCD treatments increased sharply during the first 4 days, mainly due to microbial ammonification (Santos et al. 2018). The maximum NH<sub>4</sub>-N content in all treatments was found on day 4, and the values in the P and P + DCD treatments (3.2 and 3.8 g kg<sup>-1</sup>, respectively) were significantly higher than that in the CK treatment (2.6 g kg<sup>-1</sup>). The reason for these higher values was probably that the high surface area and large number of micropores of P could adsorb NH<sub>4</sub>-N or NH<sub>3</sub>, increasing the NH<sub>4</sub>-N content. Similar results were reported by Wang et al. (2018b) for pig manure composting with biochar and zeolite and by Man et al. (2016) for food waste added composting with zeolite alone. In addition, the addition of DCD inhibited nitrification and increased the NH<sub>4</sub>-N content of the compost (Zhang et al. 2016b). Thereafter, the NH<sub>4</sub>-N content in the three treatments gradually decreased until the end of composting, and the final values were all less than 0.4 g kg<sup>-1</sup>, which is safe for the compost to be used as soil amendment (Bernal et al. 2009).

### Effect of P and DCD on the gaseous emission profile

As the main gaseous emissions during the composting process, carbonaceous gases (CO<sub>2</sub> and CH<sub>4</sub>) and nitrogenous gases (NH<sub>3</sub> and N<sub>2</sub>O) were analyzed in the present study, and their changes during the composting process are illustrated in Fig. 3.

### Changes in the CO<sub>2</sub> and CH<sub>4</sub> emission profiles

CO<sub>2</sub> production is inevitable, and its emission rate reflects the microbial activity during composting (Meng et al. 2018). In the present study, CO<sub>2</sub> emissions in all treatments sharply increased during the first 2 days, remained high from days 3–7, and then gradually decreased until the end of composting (Fig. 3a). The highest CO<sub>2</sub> emission rates in the CK and P treatments were recorded on day 3, at 26.5 and 32.1 g d<sup>-1</sup>, respectively, while the maximum rate in P + DCD was on day 5, at 28.4 g d<sup>-1</sup>. This delay could have been due to the inhibition of microbial activity by DCD (Zhang et al. 2016b). Over the whole composting process, the cumulative CO<sub>2</sub> emissions were 144, 193, and 170 g in the CK, P, and P +

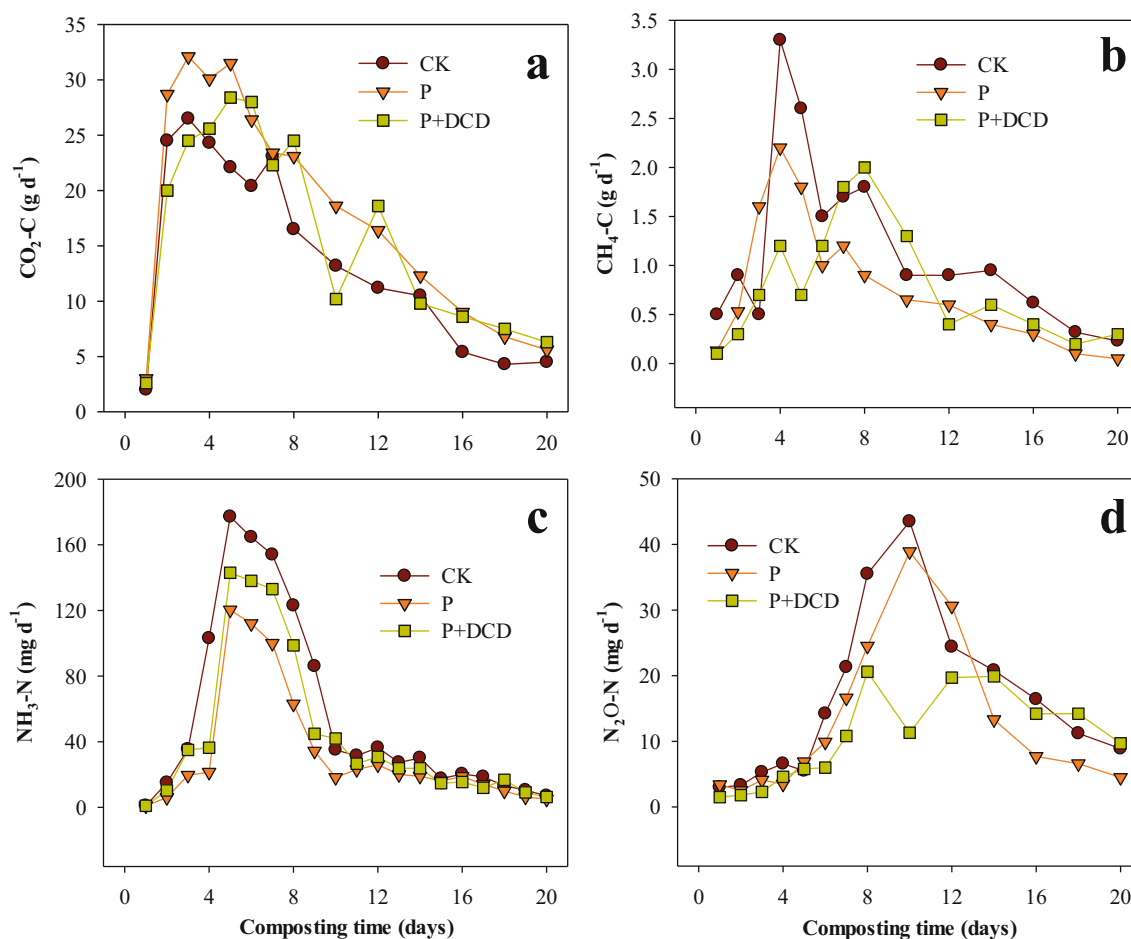


**Fig. 3** Changes in CO<sub>2</sub> (a), CH<sub>4</sub> (b), NH<sub>3</sub> (c) and N<sub>2</sub>O (d) emissions during SS composting

DCD treatments, respectively, and the emissions in the P and P + DCD treatments were increased by 34.0% and 17.6% compared with those in the CK treatment. All the differences among the treatments were significant ( $P < 0.05$ ). As an effective additive, P could increase the compost mixture porosity and the requisite microbial activity. Similar results during composting were reported by other researchers when adding similar additives, such as biochar and medical stone (Awasthi et al. 2018a; Liu et al. 2017).

The CH<sub>4</sub> emissions in the present study rapidly increased during the first 4 days (Fig. 3b), mainly due to the rapid depletion of oxygen via the decomposition of OM (Sanchez et al. 2015). At days 4 and 8, turning could have created more evenly mixed piles and eliminated the anaerobic environment; thus, the CH<sub>4</sub> emissions sharply decreased and then remained at a low level during the maturation phase. Over the whole process, the cumulative CH<sub>4</sub> emissions in the CK, P, and P + DCD treatments were 16.7, 11.5, and 15.2 g, respectively. On the one hand, the addition of P could have increased the porosity of the compost piles and microbial activity. Awasthi et al. (2016) observed that the addition of biochar and zeolite (also a bulk material, as is P) could significantly reduce CH<sub>4</sub>

emissions during SS composting. On the other hand, high NH<sub>4</sub>-N could inhibit methanogen activity and reduce CH<sub>4</sub> emissions during composting (Jiang et al. 2016). During the first 8 days, the NH<sub>4</sub>-N contents in the P and P + DCD treatments were significantly higher than those in the CK treatment (Fig. 2f). Thus, the cumulative CH<sub>4</sub> emissions in the P and P + DCD treatments were lower than those in the CK treatment by 31.5% and 33.0%, respectively.

### Changes in the NH<sub>3</sub> and N<sub>2</sub>O emission profiles

NH<sub>3</sub> emissions are the main nitrogen loss pathway during the composting process (Bernal et al. 2009). The NH<sub>3</sub> emissions increased sharply during the first 5 days, reached the highest values on day 5, decreased quickly during days 5–10, and remained at a low level until the end of composting (Fig. 3c). The maximum NH<sub>3</sub> emissions were 177.1, 120.3, and 143.0 g d<sup>-1</sup> for the CK, P, and P + DCD treatments, respectively. In addition, the cumulative NH<sub>3</sub> in the P and P + DCD treatments was reduced by 40.9% and 22.3%, respectively, compared with that in the CK treatment. The results showed that P advantageously reduces NH<sub>3</sub> emissions. DCD increased

the  $\text{NH}_4\text{-N}$  content in the P + DCD treatment due to its inhibition of nitrification (Zhang et al. 2016b); thus, the cumulative  $\text{NH}_3$  emissions in the P + DCD treatments were slightly higher than those in the P treatments. The reduction of  $\text{NH}_3$  emissions by the additive can be explained by two factors: the ability to absorb  $\text{NH}_3$ , as observed for additives such as biochar, zeolite, and bentonite (Awasthi et al. 2016; Jiang et al. 2014; Wang et al. 2018b), and the reaction of  $\text{NH}_3$  with the mineral additive to form an ammonium salt, as observed for additives such as calcium superphosphate, phosphogypsum, and phosphorus and magnesium salt (Jeong and Hwang 2005; Jiang et al. 2014, 2016). Obviously, the ability of P to reduce  $\text{NH}_3$  emissions was mainly due to the high adsorption capacity for  $\text{NH}_4\text{-N}$  and  $\text{NH}_3$  of the composting mixture.

$\text{N}_2\text{O}$ , an important GHG, is thought to have a 298-fold higher global warming potential than  $\text{CO}_2$  (IPCC 2007). During the first 5 days, the  $\text{N}_2\text{O}$  emissions in all treatments were very low (Fig. 3d), mainly because the high temperatures (Fig. 2a) limited the activity of nitrifying and denitrifying bacteria (Sanchez et al. 2015; Sommer and Møller 2000). After day 5, the  $\text{N}_2\text{O}$  emissions in all treatments rapidly increased mainly because the temperature decreased and some anaerobic pockets formed, which are conducive to the production of  $\text{CH}_4$  (Wang et al. 2016). The maximum values in CK and P were 43.5 and 38.9  $\text{mg d}^{-1}$ , respectively, on day 10, while the peak values in P + DCD were 20.6 and 38.9  $\text{mg d}^{-1}$ , respectively, on day 8. This difference was a result of the second DCD addition on day 8 in the P + DCD treatment, which inhibited nitrification and denitrification, resulting in a decrease in  $\text{N}_2\text{O}$  emissions on day 10. Over the entire experimental period, the cumulative  $\text{N}_2\text{O}$  emissions were 358.4, 284.6, and 236.7 g in the CK, P, and P + DCD treatments, respectively, and the cumulative  $\text{N}_2\text{O}$  emissions in the P and P + DCD treatments were reduced by 20.6% and 33.9% ( $P < 0.05$ ), respectively, compared with those in the CK treatment. Similar to P, Wang et al. (2018b) reported that the combined addition of zeolite and biochar reduced  $\text{N}_2\text{O}$  emissions by 37.7% compared with the addition of biochar alone during the composting of pig manure and vinegar, mainly because zeolite absorbed  $\text{N}_2\text{O}$  in the compost. In addition, P could improve the aeration by increasing the porosity and decreasing the denitrification rate. A similar result was found in a previous study by Awasthi et al. (2018a), who composted pig manure with medical stone.

Based on the profiles of  $\text{NH}_3$ ,  $\text{N}_2\text{O}$ ,  $\text{CH}_4$ , and  $\text{CO}_2$  emissions, the P + DCD treatments decreased the cumulative gaseous emissions by 22% for  $\text{NH}_3$ , 34% for  $\text{N}_2\text{O}$ , and 33.0% for  $\text{CH}_4$  compared with the control, respectively. Thus, the combined addition of peletith and dicyandiamide (DCD) was suggested for reducing the emissions of  $\text{NH}_3$  and greenhouse gases during SS composting.

## Effects of P and DCD on the composition of fungal communities

A total of 327,066 high-quality sequences were obtained from the SS composting samples in the three treatments and were clustered into 1054 fungal OTUs based on a 0.03 difference threshold. The number of OTUs of the seven samples ranged from 335 to 557, and the highest number was found in the initial SS. The number of fungal OTUs decreased after composting, which could have been a result of the environmental conditions, especially the high temperatures during the thermophilic stage, because such conditions are more restricted niches and can even eradicate fungal pathogens (Boulter et al. 2002). A similar result was reported by Wang et al. (2018a), who composted cow manure and wood chips.

The coverage (Table 2) of all samples was high at above 0.99, which validated the sequencing results and means that the data could reflect the actual characteristics of the reactors. The Chao and Ace indexes in P were higher than those in CK both during the thermophilic and maturity stage. However, the Chao and Ace indexes in P + DCD essentially the same as those in CK during the thermophilic stage but were obviously increased during the maturity stage. During the thermophilic and maturity stages, the Shannon index decreased in CK but increased in P and P + DCD, whereas the Simpson index increased in CK but decreased in P and P + DCD. Based on all the alpha diversity indexes, the addition of DCD decreased the fungal community richness and diversity during the thermophile stage because of its inhibitory effect on microorganisms. These data also supported the positive influence of P on the microbial communities and activity during the composting process. The high total pore volume and specific surface area of P created a suitable habitat and acted as a structural amendment for the growth of microorganisms, similar to biochar (Mao et al. 2018). In addition, as a mineral, P could provide inorganic nutrients to benefit the endogenous and exogenous microbial communities.

Figure 4a shows the relative abundances of fungi at the phylum and genus levels of the initial SS and composting samples. Only three fungal phyla (relative abundance of over 1%) were detected throughout the composting: *Ascomycota*, *unclassified\_k\_fungi*, and *Basidiomycota*. *Unclassified\_k\_fungi* were the dominant fungal phyla, accounting for 67 to 51% of the fungal community in the initial SS during the thermophilic stage in the three treatments. A similar result was reported by Tian et al. (2017), who found that the fungal community was dominated by *unclassified\_k\_fungi*, with an abundance of 51.4% in the initial stage during the composting of Chinese medicinal herbal residues. The relative abundance percentage of *unclassified\_k\_fungi* during the thermophilic stage in the three treatments decreased to 51%, and the values in the maturity stage in the CK, P, and P + DCD treatments were continuously reduced to 35.9%, 28.7%, and 23.1%, respectively. However, the relative abundance percentage of

**Table. 2** Observed number of OTUs, estimated indexes (Chao, Shannon and Simpson, Ace) and coverage during two sampling stages in the different treatments

| Items    | IS    | CK    |       | P     |       | P + DCD |       |
|----------|-------|-------|-------|-------|-------|---------|-------|
|          |       | (1)   | (2)   | (1)   | (2)   | (1)     | (2)   |
| OTU      | 557   | 450   | 335   | 472   | 349   | 441     | 428   |
| Chao     | 615.5 | 463.1 | 341.5 | 492.1 | 354.9 | 468.8   | 449.2 |
| Ace      | 614.7 | 465.1 | 342.4 | 492.2 | 357.7 | 462.4   | 447.4 |
| Shannon  | 3.81  | 4.28  | 4.02  | 4.15  | 4.42  | 4.06    | 4.17  |
| Simpson  | 0.078 | 0.048 | 0.049 | 0.049 | 0.023 | 0.057   | 0.045 |
| Coverage | 0.997 | 0.999 | 0.998 | 0.999 | 0.999 | 0.999   | 0.999 |

(1) indicates the 4th sample, while (2) indicates the 20th sample, OTU stands for operational taxonomic unit

*Ascomycota* gradually increased to 61.8%, 66.3%, and 72.9% in the maturity stage in the CK, P, and P + DCD treatments, and this phylum was the dominant fungal phylum at the end of composting. A similar result was found by Wang et al. (2018a), who reported that the main fungal communities were *Ascomycota* (> 90%) during the maturity stage when composting cow manure and wood chips. For *Basidiomycota* fungi, the relative abundance in the P and P + DCD treatments was significantly lower than that in the CK treatment in the thermophilic stage but significantly increased by 221% and 120% compared with that in the CK treatment during the maturity stage. *Ascomycota* and *Basidiomycota* are the main fungal decomposers in organic waste composting and their high abundance is beneficial for the degradation of OM (Neher et al. 2013; Yu et al. 2015). Thus, the addition of P and DCD accelerated the degradation of OM, and the OM profiles of the CK, P, and P + DCD treatments also support this conclusion (Fig. 2c).

At the genus level, a total of 17 genera that exceeded 1% were identified in the three treatments. As shown in Fig. 4b, the main fungal genera included *unclassified\_k\_fungi*, *Trichoderma*, *Aspergillus*, *Talaromyces*, *Penicillium*, and *Pseudeurotium*. It has been reported that *Aspergillus* can adapt to the changes in temperature, pH, and moisture

during composting, and Zhang et al. (2016c) and Tian et al. (2017) reported *Aspergillus* as the dominant genus during agricultural waste and Chinese medicinal herbal residue composting, respectively. Neher et al. (2013) found that *Talaromyces* was the dominant genus during composting of manure mixed with hardwood. *Thermomyces* has been reported by many researchers as the dominant genus during composting (Awasthi et al. 2017; Zhang et al. 2016c). However, this genus was not detected in this study. In addition, *Trichoderma* was the dominant genus in this study but was not reported by other studies during composting. These differences may be due to the different raw materials used because the physicochemical properties of raw materials have a significant effect on the environment, which ultimately affects the fungal community. *Trichoderma*, which can produce cellulases, glucanases, pectinases, and xylanases, plays a crucial role in degrading cellulose and hemicelluloses during composting (Nsereko et al. 2002).

Statistical comparison of the relative abundances showed that all of the top 10 classified fungal genera except *Guehomyces* were more abundant in P than in CK (Fig. 5a) during the thermophilic stage. However, in this stage, only three genera were more abundant in P + DCD than in CK (Fig. 5b). During the maturity stage, all

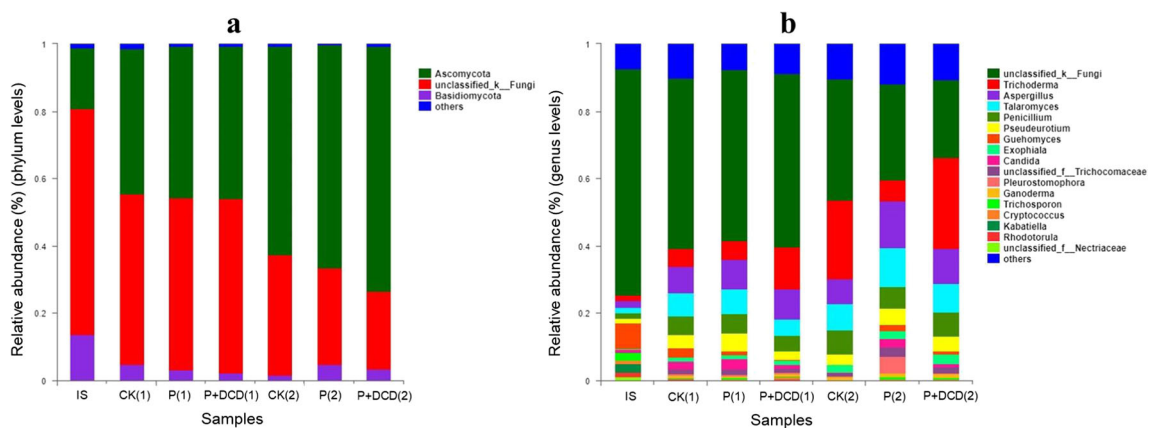


**Fig. 4** Basic information on the fungal communities during composting. **a** Phylum-level composition of the fungal communities (relative abundances exceeding 1%). **b** Relative abundances of the classified fungal

genera (relative abundances exceeding 1%) detected during cow manure composting at the genus level. (1) indicates the 4th sample, while (2) indicates the 20th sample



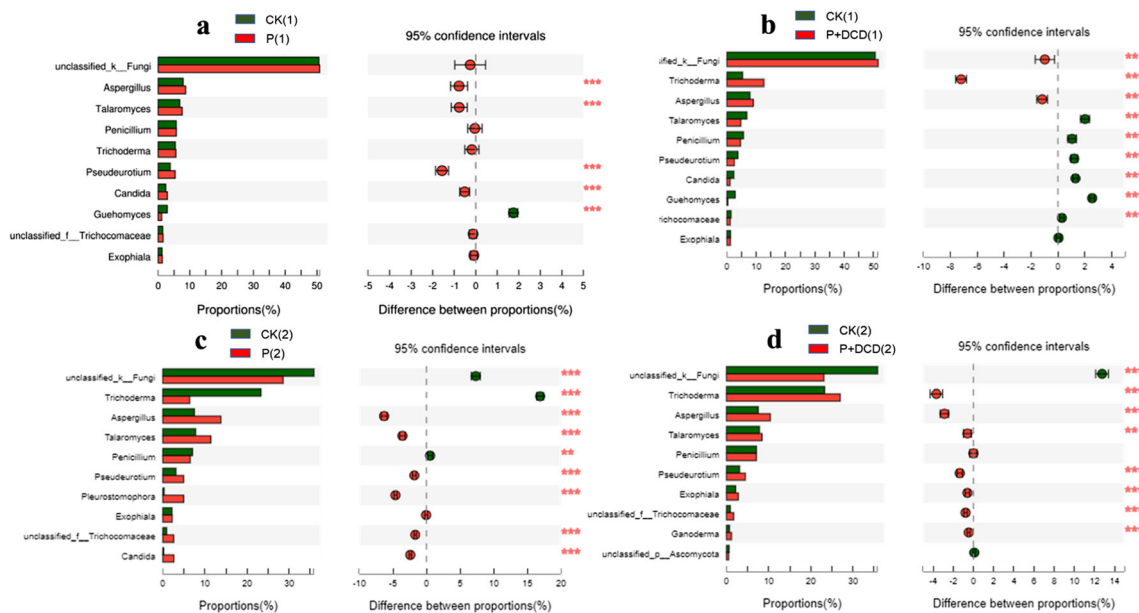


**Fig. 5** Statistical comparison of the relative abundances at the genus level. **a** Comparison of the top ten genera between CK (1) and P (1). **b** comparison of the top ten genera between CK (1) and P + DCD (1). **c** Comparison of the top ten genera between CK (2) and P (2). **d**

Comparison of the top ten genera between CK (2) and P + DCD (2). (1) indicates the 4th sample, while (2) indicates the 20th sample. Statistical analysis was performed using the Mann-Whitney *U* test. *n* = 10 in each group. \*0.01 < *P* < 0.05, \*\*0.001 < *P* < 0.001, \*\*\**P* < 0.001

of the ten top genera except for *unclassified\_k\_fungi* were more abundant in the P and P + DCD treatments than in the CK treatment. This result suggests that DCD inhibited microbial activity but did not kill microbes because DCD is a bacteriostatic agent rather than a bactericide (Luo et al. 2013). Similarly, Zhang et al. (2016b) reported that 3,4-dimethylpyrazole phosphate, also an NI, reduced the microbial richness but did not change the evolution of bacterial community diversity.

**Correlations between selected environmental factors, gaseous emissions, and fungal communities**

A correlation heat map of the relationship among the top 30 fungal genera and 6 selected environmental factors (temperature, pH, TN, NH<sub>4</sub>-N, OM, and DOC) is shown in Fig. 6a. TN showed a significant positive correlation with *Ganoderma* (*R*<sup>2</sup> = 0.829) and *Penicillium* (*R*<sup>2</sup> = 0.899) and an extremely significant positive correlation with *Talaromyces* (*R*<sup>2</sup> = 0.943) and *Exophiala*

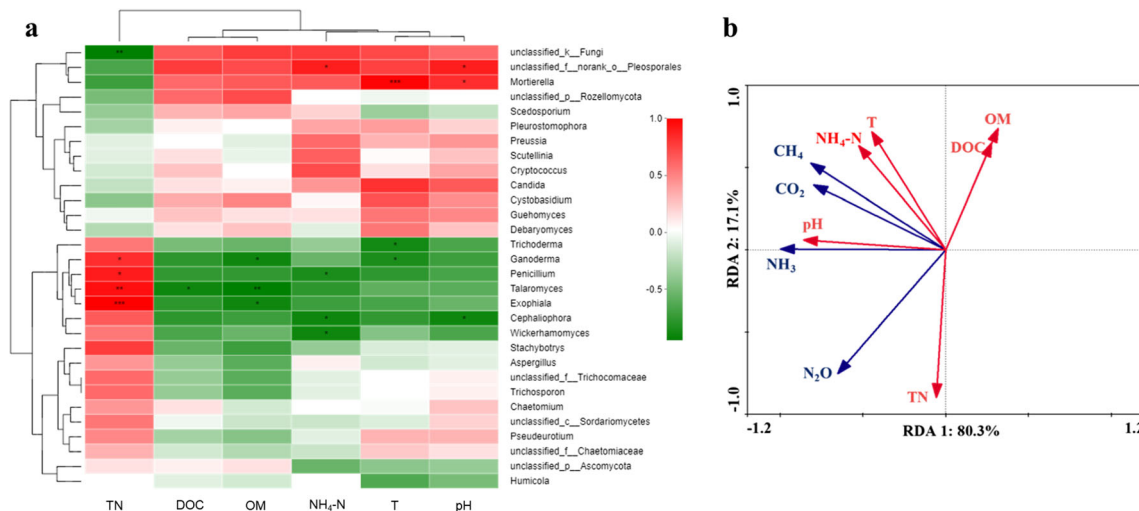


**Fig. 6** Correlations between selected environmental factors, fungal community members, and gaseous emissions. **a** Correlation heat map of the top 30 genera and environmental factors. The x- and y-axes correspond to the environmental factors and genera, respectively. R in different

colors to show, the right side of the legend is the color range of different R values. \*0.01 < *P* < 0.05, \*\*0.001 < *P* < 0.001, \*\*\**P* < 0.001. **b** RDA of physiochemical properties and gaseous emissions during SS composting

( $R^2 = 0.999$ ). In addition, TN had an extremely significant negative correlation with *unclassified\_k\_fungi* ( $R^2 = -0.943$ ). OM demonstrated a significant negative correlation with *Exophiala* ( $R^2 = -0.886$ ) and *Ganoderma* ( $R^2 = -0.886$ ) and an extremely significant negative correlation with *Talaromyces* ( $R^2 = -0.943$ ).  $\text{NH}_4\text{-N}$  was significantly negatively correlated with *Penicillium* ( $R^2 = -0.841$ ) and *Cephalophora* ( $R^2 = -0.886$ ) and *Wickerhamomyces* ( $R^2 = -0.886$ ) and significantly positively correlated with *unclassified\_f\_norank\_o\_Pleosporales* ( $R^2 = -0.886$ ). Temperature showed an extremely significant positive correlation with *Mortierella* ( $R^2 = 0.986$ ) and a significant negative correlation with *Trichoderma* ( $R^2 = -0.870$ ) and *Ganoderma* ( $R^2 = -0.841$ ). pH had a significant positive correlation with *unclassified\_f\_norank\_o\_Pleosporales* ( $R^2 = 0.886$ ) and *Mortierella* ( $R^2 = 0.829$ ) and a significant negative correlation with *Cephalophora* ( $R^2 = -0.886$ ). Wang et al. (2018a) reported that pH, temperature, and C/N could explain 57.7%, 32.0%, and 3.1% of the variation in fungal genera data, respectively, during cow manure composting. Yu et al. (2015) also found that the majority of variation in the distribution of fungal community structure could be explained by temperature, pH, and TOC during agricultural waste composting.

In addition, redundancy analysis (RDA) was also conducted to investigate the correlation between the 6 selected environmental factors and gaseous emissions ( $\text{NH}_3$ ,  $\text{CO}_2$ ,  $\text{CH}_4$ , and  $\text{N}_2\text{O}$ ) (Fig. 6b). The results showed that the first canonical axes explained 80.3%, 74.3%, and 81.8% of the variation in gaseous emissions data for the CK, P, and P + DCD treatments, respectively. The relationship between gaseous emissions and physicochemical indexes, especially temperature, pH, OM, and TN, indicated that gaseous emissions had been controlled by not only basic environmental factors but also the transformations of carbon and nitrogen. Similar results were reported by Awasthi et al. (2018a, b) during SS composting. Overall, these results indicate that temperature, pH, OM, and TN exerted the main effects on fungal activity and gaseous emissions during SS composting.

## Conclusions

This study investigated the effect of P and DCD on gaseous emissions and the fungal community. The results indicated that P could improve the composting process and accelerate OM degradation. Moreover, the addition of P and DCD effectively reduced  $\text{NH}_3$ ,  $\text{N}_2\text{O}$ , and  $\text{CH}_4$  through their unique properties. Statistical comparison of the relative abundances showed that the P and P + DCD treatments significantly increased the fungal community richness at the genus level. Temperature, pH, OM, and TN were found to be the significant variables affecting the fungal community and gaseous emissions during this study.

**Funding information** Financial support for this investigation was provided by National Natural Science Foundation of China (41805123, 51508167, and 41807327), the Key Research Project of Colleges and Universities for Education Department of Henan Province (17A610006 and 17B610006), and Natural Science Foundation of Henan Province of China (182300410153).

**Publisher's note** Springer Nature remains neutral with regard to jurisdictional claims in published maps and institutional affiliations.

## References

- Awasthi MK, Wang Q, Ren X, Zhao J, Huang H, Awasthi SK, Lahori AH, Li R, Zhou L, Zhang Z (2016) Role of biochar amendment in mitigation of nitrogen loss and greenhouse gas emission during sewage sludge composting. *Bioresour Technol* 219:270–280
- Awasthi MK, Li J, Kumar S, Awasthi SK, Wang Q, Chen H, Wang M, Ren X, Zhang Z (2017) Effects of biochar amendment on bacterial and fungal diversity for co-composting of gelatin industry sludge mixed with organic fraction of municipal solid waste. *Bioresour Technol* 246:214–223
- Awasthi MK, Wang Q, Awasthi SK, Wang M, Chen H, Ren X, Zhao J, Zhang Z (2018a) Influence of medical stone amendment on gaseous emissions, microbial biomass and abundance of ammonia oxidizing bacteria genes during biosolids composting. *Bioresour Technol* 247:970–979
- Awasthi MK, Wang Q, Chen H, Wang M, Awasthi SK, Ren X, Cai H, Li R, Zhang Z (2018b) In-vessel co-composting of biosolid: focusing on mitigation of greenhouse gases emissions and nutrients conservation. *Renew Energy* 129:814–823
- Barrington S, Choiniere D, Trigui M, Knight W (2002) Effect of carbon source on compost nitrogen and carbon losses. *Bioresour Technol* 83:189–194
- Bernal MP, Alburquerque JA, Moral R (2009) Composting of animal manures and chemical criteria for compost maturity assessment. A review. *Bioresour Technol* 100:5444–5453
- Boulter JI, Trevors JT, Boland GJ (2002) Microbial studies of compost: bacterial identification, and their potential for turfgrass pathogen suppression. *World J Microbiol Biotechnol* 18:661–671
- Chan MT, Selvam A, Wong JW (2016) Reducing nitrogen loss and salinity during 'struvite' food waste composting by zeolite amendment. *Bioresour Technol* 200:838–844
- Chowdhury MA, de Neergaard A, Jensen LS (2014) Potential of aeration flow rate and bio-char addition to reduce greenhouse gas and ammonia emissions during manure composting. *Chemosphere* 97:16–25
- Deer WA (1992) An introduction to rock-forming minerals. Longman Scientific & Technical 66:509–517
- Edgar RC (2010) Search and clustering orders of magnitude faster than BLAST. *Bioinformatics* 26:2460–2461
- Gomez-Brandon M, Lazcano C, Dominguez J (2008) The evaluation of stability and maturity during the composting of cattle manure. *Chemosphere* 70:436–444
- Groat LE (1992) The chemistry of vesuvianite. *Can Mineral* 30:19–48
- Haddadin MS, Haddadin J, Arabiyat OI, Hattar B (2009) Biological conversion of olive pomace into compost by using *Trichoderma harzianum* and *Phanerochaete chrysosporium*. *Bioresour Technol* 100:4773–4782
- IPCC (2007) Climate change 2007: impacts, adaptation and vulnerability. Contribution of working group II to the fourth assessment report of the intergovernmental panel on climate change. Cambridge University Press, Cambridge
- Jain MS, Jambhulkar R, Kalamdhad AS (2018) Biochar amendment for batch composting of nitrogen rich organic waste: effect on degradation kinetics, composting physics and nutritional properties. *Bioresour Technol* 253:204–213

- Jeong YK, Hwang SJ (2005) Optimum doses of Mg and P salts for precipitating ammonia into struvite crystals in aerobic composting. *Bioresour Technol* 96:1–6
- Jiang J, Huang Y, Liu X, Huang H (2014) The effects of apple pomace, bentonite and calcium superphosphate on swine manure aerobic composting. *Waste Manag* 34:1595–1602
- Jiang T, Ma X, Tang Q, Yang J, Li G, Schuchardt F (2016) Combined use of nitrification inhibitor and struvite crystallization to reduce the  $\text{NH}_3$  and  $\text{N}_2\text{O}$  emissions during composting. *Bioresour Technol* 217:210–218
- Jiang J, Kang K, Chen D, Liu N (2017) Impacts of delayed addition of N-rich and acidic substrates on nitrogen loss and compost quality during pig manure composting. *Waste Manag* 72:161–167
- Jiang J, Kang K, Wang C, Sun X, Dang S, Wang N, Wang Y, Zhang C, Yan G, Li Y (2018) Evaluation of total greenhouse gas emissions during sewage sludge composting by the different dicyandiamide added forms: mixing, surface broadcasting, and their combination. *Waste Manag* 81:94–103
- Kelliher FM, Clough TJ, Clark H, Rys G, Sedcole JR (2008) The temperature dependence of dicyandiamide (DCD) degradation in soils: a data synthesis. *Soil Biol Biochem* 40:1878–1882
- Khan E, Khaodhir S, Ruangrote D (2009) Effects of moisture content and initial pH in composting process on heavy metal removal characteristics of grass clipping compost used for stormwater filtration. *Bioresour Technol* 100:4454–4461
- Khan N, Clark I, Sánchez-Monedero MA, Shea S, Meier S, Bolan N (2014) Maturity indices in co-composting of chicken manure and sawdust with biochar. *Bioresour Technol* 168:245–251
- Kulikowska D (2016) Kinetics of organic matter removal and humification progress during sewage sludge composting. *Waste Manag* 49:196–203
- Lam SK, Suter H, Mosier AR, Chen D (2016) Using nitrification inhibitors to mitigate agricultural  $\text{N}_2\text{O}$  emission: a double-edged sword? *Glob Chang Biol* 23:485–489
- Li H, Ru J, Yin W, Liu X, Wang J, Zhang W (2009) Removal of phosphate from polluted water by lanthanum doped vesuvianite. *J Hazard Mater* 168(1):326–330
- Li YB, Jin PF, Liu TT, Lv JH, Jiang JS (2018) A novel method for sewage sludge composting using bamboo charcoal as a separating material. *Environ Sci Pollut Res* 1–12
- Liu N, Zhou J, Han L, Ma S, Sun X, Huang G (2017) Role and multi-scale characterization of bamboo biochar during poultry manure aerobic composting. *Bioresour Technol* 241:190–199
- Luo Y, Li G, Luo W, Schuchardt F, Jiang T, Xu D (2013) Effect of phosphogypsum and dicyandiamide as additives on  $\text{NH}_3$ ,  $\text{N}_2\text{O}$  and  $\text{CH}_4$  emissions during composting. *J Environ Sci* 25:1338–1345
- Man TC, Selvam A, Wong JWC (2016) Reducing nitrogen loss and salinity of “struvite” food waste composting by zeolite amendment. *Bioresour Technol* 200:838–844
- Mao H, Lv Z, Sun H, Li R, Zhai B, Wang Z, Awasthi MK, Wang Q, Zhou L (2018) Improvement of biochar and bacterial powder addition on gaseous emission and bacterial community in pig manure compost. *Bioresour Technol* 258:195–202
- Meng L, Li W, Zhang S, Wu C, Lv L (2017) Feasibility of co-composting of sewage sludge, spent mushroom substrate and wheat straw. *Bioresour Technol* 226:39–45
- Meng L, Zhang S, Gong H, Zhang X, Wu C, Li W (2018) Improving sewage sludge composting by addition of spent mushroom substrate and sucrose. *Bioresour Technol* 253:197–203
- Metcalf JL, Xu ZZ, Weiss S, Lax S, Van TW, Hyde ER, Song SJ, Amir A, Larsen P, Sangwan N (2016) Microbial community assembly and metabolic function during mammalian corpse decomposition. *Science* 351:158–162
- Neher DA, Weicht TR, Bates ST, Leff JW, Fierer N (2013) Changes in bacterial and fungal communities across compost recipes, preparation methods, and composting times. *PLoS One* 8:e79512
- Nsereko VL, Beauchemin KA, Morgavi DP, Rode LM, Furtado AF, Mcallister TA, Iwaasa AD, Yang WZ, Wang Y (2002) Effect of a fibrolytic enzyme preparation from *Trichoderma longibrachiatum* on the rumen microbial population of dairy cows. *Can J Microbiol* 48:14–20
- Pan Y, Tian S, Zhao Y, Zhang L, Zhu X, Gao J, Huang W, Zhou Y, Song Y, Zhang Q (2018) Identifying ammonia hotspots in China using a national observation network. *Environ Sci Technol* 52:3926–3934
- Sanchez A, Artola A, Font X, Gea T, Barrena R, Gabriel D, Sanchez-Monedero MA, Roig A, Cayuela ML, Mondini C (2015) Greenhouse gas emissions from organic waste composting. *Environ Chem Lett* 13:223–238
- Santos C, Goufo P, Fonseca J, Pereira JLS, Ferreira L, Coutinho J, Trindade H (2018) Effect of lignocellulosic and phenolic compounds on ammonia, nitric oxide and greenhouse gas emissions during composting. *J Clean Prod* 171:548–556
- Sommer SG, Möller HB (2000) Emission of greenhouse gases during composting of deep litter from pig production-effect of straw content. *J Agric Sci* 134:327–335
- Tian X, Yang T, He J, Chu Q, Jia X, Huang J (2017) Fungal community and cellulose-degrading genes in the composting process of Chinese medicinal herbal residues. *Bioresour Technol* 241:374–383
- Tortosa G, Castellano-Hinojosa A, Correa-Galeote D, Bedmar EJ (2016) Evolution of bacterial diversity during two-phase olive mill waste (“alperujo”) composting by 16S rRNA gene pyrosequencing. *Bioresour Technol* 224:101–111
- Wang Q, Wang Z, Awasthi MK, Jiang Y, Li R, Ren X, Zhao J, Shen F, Wang M, Zhang Z (2016) Evaluation of medical stone amendment for the reduction of nitrogen loss and bioavailability of heavy metals during pig manure composting. *Bioresour Technol* 220:297–304
- Wang K, Yin X, Mao H, Chu C, Tian Y (2018a) Changes in structure and function of fungal community in cow manure composting. *Bioresour Technol* 255:123–130
- Wang Q, Awasthi MK, Ren X, Zhao J, Li R, Wang Z, Wang M, Chen H, Zhang Z (2018b) Combining biochar, zeolite and wood vinegar for composting of pig manure: the effect on greenhouse gas emission and nitrogen conservation. *Waste Manag* 74:221–230
- Wei H, Wang L, Hassan M, Xie B (2018) Succession of the functional microbial communities and the metabolic functions in maize straw composting process. *Bioresour Technol* 256:333–341
- Yang F, Li G, Shi H, Wang Y (2015) Effects of phosphogypsum and superphosphate on compost maturity and gaseous emissions during kitchen waste composting. *Waste Manag* 36:70–76
- Yu M, Zhang J, Xu Y, Xiao H, An W, Xi H, Xue Z, Huang H, Chen X, Shen A (2015) Fungal community dynamics and driving factors during agricultural waste composting. *Environ Sci Pollut Res* 22:19879–19886
- Zhang J, Chen M, Sui Q, Tong J, Jiang C, Lu X, Zhang Y, Wei Y (2016a) Impacts of addition of natural zeolite or a nitrification inhibitor on antibiotic resistance genes during sludge composting. *Water Res* 91:339–349
- Zhang J, Sui Q, Li K, Chen M, Tong J, Qi L, Wei Y (2016b) Influence of natural zeolite and nitrification inhibitor on organics degradation and nitrogen transformation during sludge composting. *Environ Sci Pollut Res* 23:1324–1334
- Zhang L, Zhang H, Wang Z, Chen G, Wang L (2016c) Dynamic changes of the dominant functioning microbial community in the compost of a 90-m<sup>3</sup> aerobic solid state fermentor revealed by integrated metabolomics. *Bioresour Technol* 203:1–10
- Zhang B, Wang MM, Wang B, Xin Y, Gao J, Liu H (2018) The effects of bio-available copper on macrolide antibiotic resistance genes and mobile elements during tylosin fermentation dregs co-composting. *Bioresour Technol* 251:230–237